

# Low-temperature sintering of zinc oxide varistors

MOHAMED N. RAHAMAN

*University of Missouri-Rolla, Ceramic Engineering Department, Rolla, Missouri 65401, USA*

LUTGARD C. DE JONGHE

*Lawrence Berkeley Laboratory, Center for Advanced Materials, Materials and Chemical Sciences Division and Department of Materials Science and Mineral Engineering, University of California, Berkeley, California 94720, USA*

JAMES A. VOIGT, BRUCE A. TUTTLE

*Sandia National Laboratories, Albuquerque, New Mexico 87185, USA*

High-field varistors in the system ZnO–CoO–MnO–Bi<sub>2</sub>O<sub>3</sub> were fabricated using powders prepared by a previously developed coprecipitation process. Following calcination, the powders were compacted and densified by conventional pressureless sintering at temperatures below 750°C in air. The effects of sample green density, sintering temperature, and grain-growth inhibitor on densification and microstructure development were investigated. Addition of aluminium at the 125 p.p.m level was used to inhibit grain growth. Samples with densities >0.98 theoretical and grain sizes <1 μm were fabricated by high-pressure cold-isostatic pressing followed by sintering at 730°C. For comparison, typical commercial varistor devices have grain sizes of about 20 μm and switching fields of approximately 2 kV cm<sup>-1</sup> after sintering at 1200 to 1400°C. As a result of the fine grain size, our high-field varistors had switching fields of 45 kV cm<sup>-1</sup> at a current density of 10 A cm<sup>-2</sup>. Consistent with earlier work on extremely high-density varistors (>0.98 theoretical) prepared from similar powders, nonlinearity coefficients of about 10 were measured for current densities between 2.5 and 10 A cm<sup>-2</sup>.

## 1. Introduction

Metal oxide varistors formed by sintering a mixture of ZnO with small additions of Bi<sub>2</sub>O<sub>3</sub> and other oxides constitute a novel class of electronic materials that exhibit the basic property of highly nonlinear current-voltage characteristics. In general, the functional dependence of the current density,  $J$ , on the electric field,  $E$ , in the varistor's nonlinear region can be described by an equation of the form

$$J = kE^\alpha \quad (1)$$

where  $k$  is a constant, and  $\alpha$ , referred to as the non-linearity coefficient, varying from 2 to 50. For a given varistor material,  $\alpha$  is not a constant but goes through a maximum as  $J$  is increased. Zinc oxide varistors have found numerous applications as voltage regulators and transient voltage suppressors in electronic devices. In operation, the varistor is connected between the power source and the ground; when the electric field exceeds the switching field,  $E_s$ , the surge is carried away through the varistor, thus protecting the circuit. It is therefore desirable to control varistor characteristics in order to optimize specific protection needs and device size requirements.

Numerous investigators [1–13] have studied the effects of processing and microstructure on electrical

conduction in ZnO varistors. The non-linear current-voltage characteristic is achieved by doping with Bi<sub>2</sub>O<sub>3</sub> and any of several oxides, including CoO, MnO, Cr<sub>2</sub>O<sub>3</sub>, Sb<sub>2</sub>O<sub>3</sub> and SnO<sub>2</sub>. It is generally believed [1, 14–20] that doping results in the formation of electrostatic barriers at the grain boundaries with characteristic voltage drops of 2 to 4 V per grain boundary [21, 22]. The increase in conductivity has been attributed to the temporary breakdown or lowering of the electrostatic barriers. The actual mechanism of breakdown has been explained as being due to the breakdown of charge-depletion layers or to electron tunnelling (see, for example, a review by Levinson and Philipp [14]).

Most previous work on fabrication of ZnO varistors has utilized conventional, pressureless sintering at 1200 to 1400°C for up to 24 h, or hot pressing. For the fabrication of high switching field (>10 kV cm<sup>-1</sup>) varistors, one main disadvantage of the elevated temperature sintering process is liquid formation and pronounced grain growth [23]. Zinc oxide varistors fabricated by elevated temperature sintering generally have grain sizes of 5 to 20 μm. Thus, the devices used in high-voltage applications (>1 kV) tend to be large. In order to reduce grain growth during densification, a number of researchers have utilized hot-pressing

techniques. Snow *et al.* [8] prepared ZnO varistors using conventional mixing techniques followed by hot pressing in an oxidizing atmosphere. Samples that were hot pressed below  $\sim 850^\circ\text{C}$  contained almost zero porosity and had grain sizes of  $< 1\ \mu\text{m}$ . The switching field and  $\alpha$  were typically  $> 10\ \text{kV cm}^{-1}$  and 20, respectively. Lauf and Bond [10] used a sol-gel processing technique to prepare the doped ZnO powders, followed by vacuum hot pressing below  $800^\circ\text{C}$ . The fabricated samples were subjected to subsequent heat treatment in air at temperatures between 700 and  $1000^\circ\text{C}$  to develop their varistor properties. The electrical properties were found to be dependent on the initial hot-pressing temperature and the subsequent heat-treatment temperature. Samples that were heat treated at  $1000^\circ\text{C}$  showed  $E_s$  values of 1.5 to  $10\ \text{kV cm}^{-1}$  and  $\alpha$  values of 25 to 40 with average grain sizes of 3 to  $5\ \mu\text{m}$ .

Dosch *et al.* [24] developed an aqueous coprecipitation process to prepare highly active doped ZnO powders that when sintered at temperatures below  $750^\circ\text{C}$  produced varistors with  $E_s > 40\ \text{kV cm}^{-1}$  and  $\alpha < 30$ ; further work on these highly active powders has been performed by Gardner and Lockwood [25, 26] and Kimball and Doughty [27]. The objective of this study was to investigate the densification characteristics of powders produced by this process. In order to reduce grain growth and maintain the high-field properties, sintering temperature was chosen to be below  $750^\circ\text{C}$ . High-temperature X-ray diffraction, dilatometry and TEM analysis of quenched varistors ( $710$  to  $750^\circ\text{C}$ ) indicate that a liquid phase is highly likely below  $750^\circ\text{C}$ . The breakdown field and the non-linear exponent of the fabricate samples were measured; however, the optimization of the electrical properties with processing and microstructure development will be the subject of a future study.

## 2. Experimental procedure

Doped ZnO powders in the system ZnO-CoO-MnO-Bi<sub>2</sub>O<sub>3</sub> were prepared by the method developed by Dosch *et al.* [24, 25]. Basically, an aqueous solution of the chloride salts of zinc, cobalt and manganese of the desired stoichiometry were hydrolysed with a NaOH solution. The hydrous oxide coprecipitate was converted to mixed oxalates by adding a solution of oxalic acid. The oxalates were calcined and then bismuth was precipitated on the surface of the resulting oxide by a local hydrolysis reaction, followed by drying. The dopants consisted of 0.56 mol % Bi<sub>2</sub>O<sub>3</sub>, 0.25 mol % CoO, and 0.25 mol % MnO. A second powder was prepared that contained, in addition, 125 p.p.m. Al as a grain-growth inhibitor [27]. Samples of the doped powders were compacted under three different conditions to obtain powders of different green densities for investigations on the effect of powder packing. First, the powders were ground lightly in a mortar and pestle and pressed uniaxially in a die at  $\sim 10\ \text{MPa}$  to give samples (10 mm diameter by 5 mm) with a relative density of 0.48. Higher uniaxially applied pressures produced laminated cracks in the samples. Second, the die-compacted samples were pressed isostatically at  $\sim 800\ \text{MPa}$  to increase the density to 0.70. Third, the

powders were milled while dispersed in toluene, in a polyethylene container using high-purity zirconia balls as a milling medium. After drying, the powders were pressed uniaxially in a die at 15 MPa to produce samples with a relative density of 0.60.

Sintering was performed initially at a constant heating rate of  $4^\circ\text{C min}^{-1}$  up to  $750^\circ\text{C}$  to investigate the dependence of the densification rate on temperature. Subsequently, most sintering experiments were performed at  $730^\circ\text{C}$ . The isothermal sintering temperature was reaching in  $\sim 8\ \text{min}$ . A two-stage sintering process was also used; the sample was first sintered isothermally at  $660^\circ\text{C}$  for 1 to 5 h followed immediately by a second isothermal sintering step at  $730^\circ\text{C}$  for up to 3 h. All sintering experiments were carried out in flowing dry air ( $50\ \text{cm}^3\ \text{min}^{-1}$ ).

The mass and dimensions of the samples were measured before and after sintering and the final densities were verified using Archimedes method. The average grain size of the sintered samples was estimated from scanning electron micrographs of fracture surfaces. Data for the electrical properties were obtained from standard d.c. resistivity measurements over the range of current densities from  $10^{-6}$  to  $10^{-3}\ \text{A cm}^{-2}$ . Pulse measurements were used for current densities ranging from 0.1 to  $10\ \text{A cm}^{-2}$ . The non-linear exponent,  $\alpha$ , was calculated from Equation 2 for the desired current densities

$$\alpha = \log(J_2/J_1)/\log(E_2/E_1) \quad (2)$$

## 3. Results and discussion

### 3.1. Densification and microstructural development

Doped ZnO powder (0.56 mol % Bi<sub>2</sub>O<sub>3</sub>, 0.25 mol % CoO, and 0.25 mol % MnO) containing 125 p.p.m. Al (used as a grain-growth inhibitor) were used in the experiments to study the effects of green density, sintering temperature and heating schedule. The results will be discussed separately in the following sections.

#### 3.1.1. Constant heating rate sintering

Fig. 1 shows the axial shrinkage,  $\Delta L/L_0$ , plotted against temperature for a sample sintered at a constant heating rate of  $4^\circ\text{C min}^{-1}$  up to  $750^\circ\text{C}$  ( $L_0$  = initial length,  $\Delta L = L_0 - L$ , where  $L$  is the instantaneous length). The initial density of the sample was 0.48, based on the calculated theoretical density of  $5.64\ \text{g cm}^{-3}$  for the doped powder. It is seen that the shrinkage (i.e. densification) rate is appreciable above  $\sim 710^\circ\text{C}$  (denoted as Region II in Fig. 1). An interesting feature of the results is an initial increase in the shrinkage rate at  $\sim 650^\circ\text{C}$ , referred to as Region I. This increase may be due to a presently unknown chemical reaction between the powder constituents that leads to the formation of a pre-eutectic liquid phase. It is also seen from Fig. 1 that a convenient temperature for isothermal sintering experiments is  $730^\circ\text{C}$ , which is somewhat below the reported ZnO-Bi<sub>2</sub>O<sub>3</sub> eutectic temperature ( $750^\circ\text{C}$ ), and at which temperature the densification rate is appreciable.

All further sintering experiments were performed isothermally; most experiments were conducted at

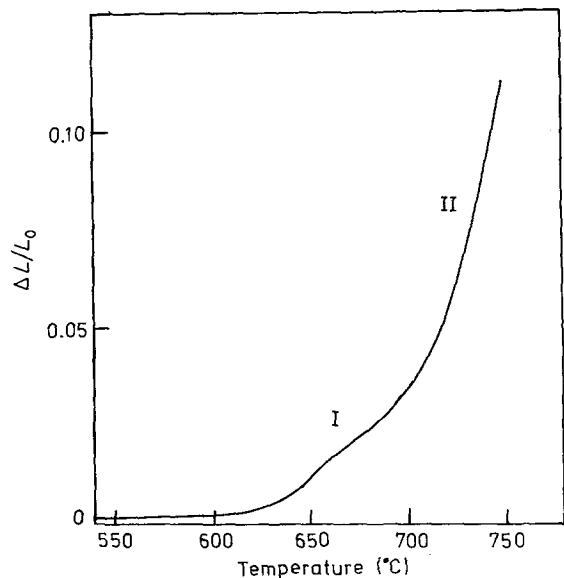


Figure 1 Axial shrinkage plotted against temperature for doped ZnO powder compacts (0.56 mol%  $\text{Bi}_2\text{O}_3$ , 0.25 mol%  $\text{CoO}$ , and 0.25 mol%  $\text{MnO}$ ) containing 125 p.p.m. Al and sintered at a constant heating rate of  $4^\circ\text{C min}^{-1}$  up to  $750^\circ\text{C}$  in air.

$730^\circ\text{C}$ , but a few were also conducted at  $715^\circ\text{C}$  for comparison.

### 3.1.2. Effect of green density

Fig. 2 shows the data for the relative density,  $\rho$ , plotted against time,  $t$ , for samples having green densities of 0.48, 0.59, and 0.70, respectively, and sintered at  $730^\circ\text{C}$ . The sintering temperature was reached in  $\sim 8$  min, and was maintained to within  $\pm 2^\circ\text{C}$  during the course of an experiment. The sintered density increases almost linearly with green density. Similar behaviour has been observed [28] for undoped, commercial powder ZnO powder sintered at  $715^\circ\text{C}$ .

The increase in sintered density with increasing green density can be understood in terms of an increase in the packing density. This, in turn, leads to an increase in the volume fraction of pores having a grain coordination number below the critical value for

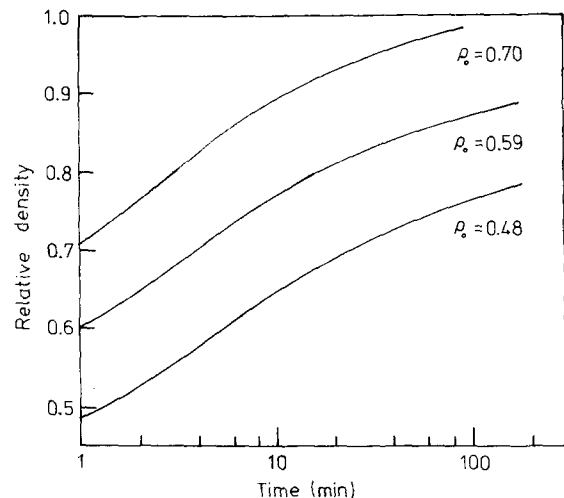


Figure 2 Relative density plotted against time for samples of three different green densities sintered isothermally at  $730^\circ\text{C}$  in air; the powder composition is described in Fig. 1.

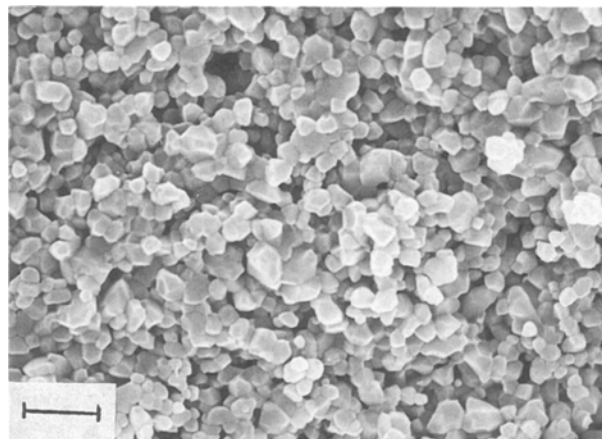


Figure 3 Scanning electron micrograph of the fracture surface of a sample sintered to a density of  $\sim 0.86$  showing pores with large grain coordination numbers. The green density of the sample was  $\sim 0.55$  and the powder composition is described in Fig. 1.

pore shrinkage. As is seen in Fig. 3, the scanning electron micrograph of the fracture surface of a sample (initial density  $\sim 0.55$ ) sintered to a density of  $\sim 0.86$  shows a number of pores with quite large coordination number. Further densification of this sample would require prolonged sintering accompanied by extensive grain growth.

A notable feature of the data is the sample pressed isostatically to a green density of 0.70 and sintered to a density of  $> 0.98$  after only 1.5 h. The high green density suggests that most of the agglomerates present in the powder were relatively soft and thus easily disrupted mechanically during cold isostatic pressing.

### 3.1.3. Effect of isothermal sintering temperature

In addition to the isothermal sintering experiments at  $730^\circ\text{C}$ , a few additional experiments were performed at  $715^\circ\text{C}$  to determine whether the sintering temperature could be lowered without causing a pronounced reduction in the sintered density. Fig. 4 compares the

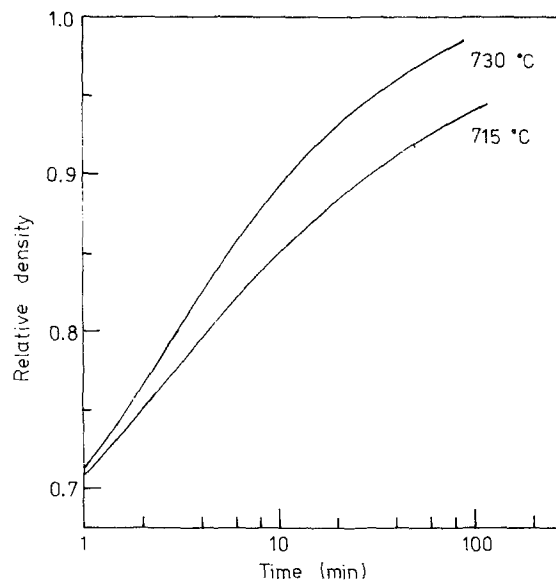


Figure 4 Relative density plotted against time for the powder composition described in Fig. 1 and sintered isothermally in air at  $715^\circ\text{C}$  and  $730^\circ\text{C}$ ; the green density of the samples was 0.70.

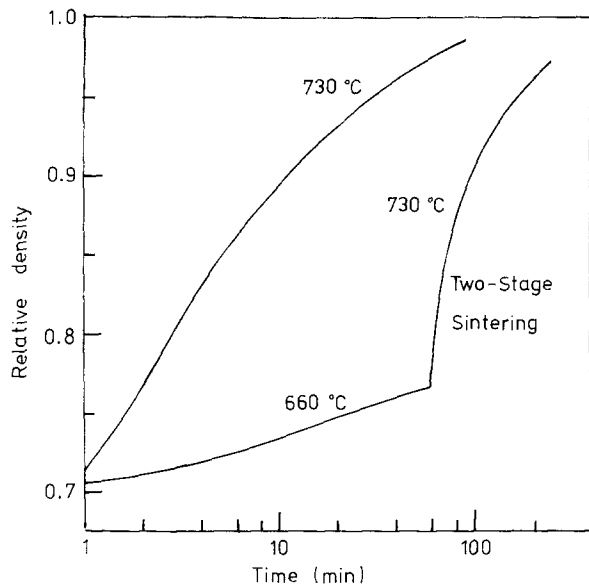


Figure 5 Relative density plotted against time for the powder composition described in Fig. 1 and sintered according to two different heating schedules: one sample was densified using a two-stage isothermal sintering schedule of 1 h at 660°C followed immediately by 2 h at 740°C, and the other was sintered isothermally at 730°C. The green density of the samples was 0.70.

densities of two samples, initial density 0.70, sintered at 730 and 715°C, respectively. The samples sintered at 716°C reached a density of 0.94 after 2 h, compared with a density of >0.98 for the sample sintered at 740°C for 1.5 h. There was no appreciable difference in the average grain sizes of the two samples. Thus, it appears that in order to achieve near theoretical density coupled with submicrometre grain size an isothermal sintering temperature of ~730°C is appropriate for the densification of these powders.

### 3.1.4. Effect of heating schedule: two-stage sintering

As seen in Fig. 1, the shrinkage rate of the doped ZnO powders shows an initial notable increase at ~650°C, followed by a more marked increase above ~710°C. Chemical reaction between the powder constituents might be responsible for the increase at ~650°C. High-temperature X-ray diffraction experiments at 700°C show crystalline Bi<sub>2</sub>O<sub>3</sub> no longer remain (at 600°C, crystalline Bi<sub>2</sub>O<sub>3</sub> is observable). A two-stage isothermal sintering experiment was performed to determine the effect of an initial soaking at 650°C on the densification and microstructural development at 730°C, and the resulting electrical properties.

Fig. 5 shows the relative density versus time for the sample densified using a two-stage isothermal sintering schedule of 1 h at 660°C followed by 2 h at 730°C compared with that for the sample sintered isothermally for 1.5 h at 730°C. The green density of the samples was 0.7. The two-stage sintering schedule produced a sample with a density of >0.97 compared with a value of >0.98 for the sample sintered isothermally at 730°C.

There was almost no difference between the microstructures of the two samples. Increasing the soaking time at 660°C led to a reduction in the final sintered density.

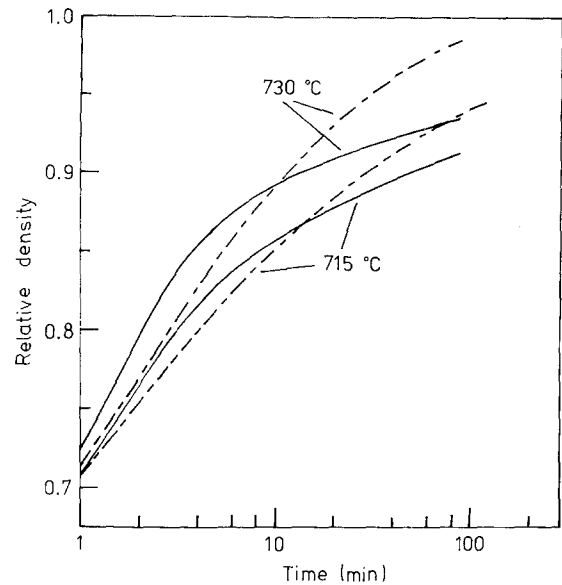


Figure 6 Relative density plotted against time for doped ZnO powders (---) with 125 p.p.m. Al or (—) without Al, that were sintered at the two temperatures shown.

### 3.1.5. Effect of aluminium

To study the effect of aluminium, which was used as a grain-growth inhibitor, doped ZnO powder compacts (initial density 0.70) containing 0 to 125 p.p.m. Al were sintered at 730 and 715°C. The results are shown in Fig. 6, where the relative density is plotted against time. It is seen that at both temperatures, the densification rates of the samples containing no aluminium were, initially, higher than those for the samples containing aluminium, but after 5 to 10 min they decreased markedly. After sintering under identical conditions, i.e. for 1.5 h at 730°C, the density of the sample containing no Al (referred to as sample A) was 0.93 compared with a value of >0.98 for the sample containing Al (sample B).

The scanning electron micrographs of the fracture surfaces of samples A and B are shown in Figs 7a and b, respectively. The effectiveness of aluminium in controlling grain growth is very apparent and similar to the results of Kimball and Doughty [27]. Sample A shows extensive grain growth (average grain size >3 μm) and some evidence of pore breakaway. Sample B, however, shows a nearly equiaxed grain morphology with an average grain size of <1 μm and no evidence of pore breakaway. For the sample containing no aluminium, reducing the sintering temperature to 715°C did not result in any appreciable reduction in the grain-growth rate or in the extent of pore breakaway. Thus, for achieving high density (>0.95) with nearly uniform submicrometre grain size by conventional sintering of the powder composition used, it is seen that the incorporation of a grain growth inhibitor is essential.

### 3.2. Electrical properties

The switching field and nonlinearity coefficient were measured for two samples; one was sintered isothermally for 2 h at 730°C, and the other was sintered using a two-stage isothermal schedule of 1 h at 660°C followed immediately by 2 h at 730°C. The green

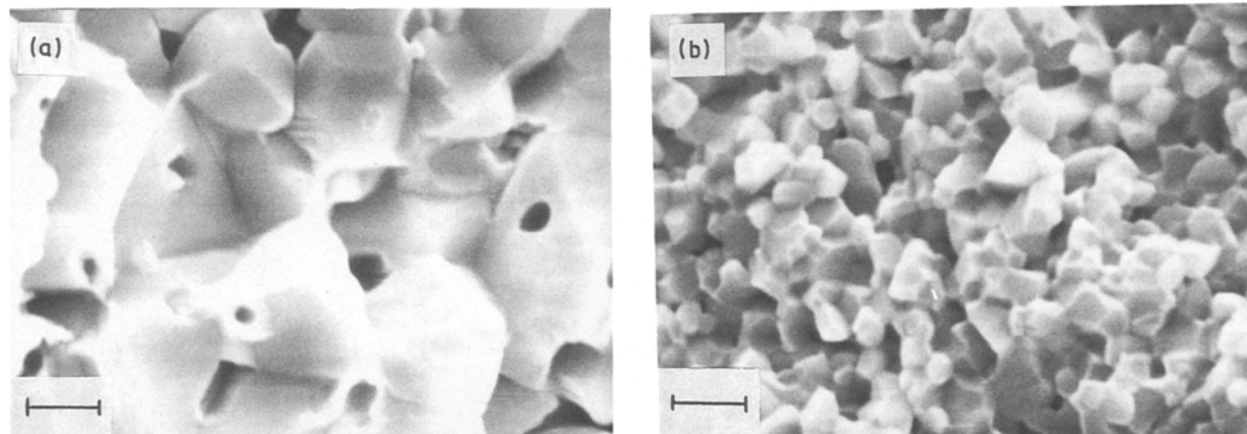


Figure 7 Scanning electron micrographs of the fracture surfaces of two doped ZnO powder compacts (green density 0.70) sintered under identical conditions, i.e. for 1.5 h at 730°C: sample A contained no  $\text{Al}_2\text{O}_3$  while sample B contained 125 p.p.m.  $\text{Al}_2\text{O}_3$ .

density and sintered density of both samples were 0.70 and  $> 0.98$ , respectively, and their initial dimensions were 16 mm diameter by 10 mm. The microstructures of the sintered samples were similar to that of Fig. 7b.

The  $E_s$  and  $\alpha$  values for both samples were  $45 \text{ kV cm}^{-1}$  (at  $10 \text{ A cm}^{-2}$ ) and  $\sim 10$  (measured between  $2.5$  and  $10 \text{ A cm}^{-2}$ ), respectively. The  $E_s$  value was ideal for the intended application but  $\alpha$  was about half the required value. The relatively low  $\alpha$  values in varistors prepared from similarly processed powders have been seen in thick ( $> 1 \text{ cm}$ ), high-density samples in a previous study by Gardner and Lockwood [26]. Further work on the optimization of the microstructure and properties of the sintered samples are in progress.

#### 4. Conclusions

Chemically prepared zinc oxide powder doped with 0.56 mol %  $\text{Bi}_2\text{O}_3$ , 0.25 mol %  $\text{CoO}$ , and 0.25 mol %  $\text{MnO}$  was conventionally sintered to  $> 0.98$  theoretical density in air at 730°C. The sintered samples showed a nearly equiaxed grain morphology with an average grain size of  $< 1 \mu\text{m}$ . The incorporation of  $\sim 125$  p.p.m. Al as a grain-growth inhibitor, and the use of high-pressure cold-isostatic pressing to increase the green packing density resulted in a high-density ( $> 98\%$ ) varistor with submicrometre grain size.

The switching field (at  $10 \text{ A cm}^{-2}$ ) for the sintered samples was  $45 \text{ kV cm}^{-1}$  and a non linearly coefficient of approximately 10 was measured. Further work is required to optimize the density, microstructure, and electrical properties of these high-field zinc oxide varistors fabricated by pressureless sintering below 750°C.

#### Acknowledgements

This work was supported by the Division of Materials Sciences, Office of Basic Energy Sciences, US Department of Energy, under Contract No. 1 DE-AC03-76F00098. At the time the work was performed, Dr M. N. Rahaman was Visiting Staff Scientist in the Materials and Chemical Sciences Division of the Lawrence Berkeley Laboratory. K. M. Kimball and M. Y. Chu are thanked for their help in powder synthesis and the micrograph shown in Fig. 3, respectively.

#### References

1. M. MATSOUKA, *Jpn. J. Appl. Phys.* **10** (1971) 736.
2. W. G. MORRIS, *J. Amer. Ceram. Soc.* **56** (1973) 360.
3. J. WONG, *ibid.* **57** (1974) 357.
4. J. WONG and W. G. MORRIS, *Amer. Ceram. Bull.* **53** (1974) 816.
5. *Idem.* *J. Appl. Phys.* **46** (1975) 1553.
6. M. INADA, *Jpn. J. Appl. Phys.* **18** (1979) 1439.
7. A. T. SANTHANAM, T. K. GUPTA and W. CARLSON, *J. Appl. Phys.* **50** (1979) 852.
8. G. S. SNOW, S. S. WHITE, R. A. COOPER and J. R. ARMIJO, *Amer. Ceram. Soc. Bull.* **59** (1980) 617.
9. J. WONG, *J. Appl. Phys.* **51** (1980) 4453.
10. R. J. LAUF and W. D. BOND, *Amer. Ceram. Soc. Bull.* **63** (1984) 278.
11. T. TAKEMURA, M. KOBAYASHI, Y. TAKADA and K. SATO, *J. Amer. Ceram. Soc.* **69** (1986) 430.
12. *Idem.* *ibid.* **70** (1987) 237.
13. T. ASOKAN, G. N. K. IYENGAR and G. R. NAGABHUSHANA, *ibid.* **70** (1987) 653.
14. L. M. LEVINSON and H. R. PHILIPP, "Application and Characterization of ZnO Varistors", in "Ceramic Materials for Electronics", edited by R. C. Buchanan (Marcel Dekker, New York, 1986).
15. J. D. LEVINE, *CRC Crit. Rev. Solid State Sci.* **5** (1975) 597.
16. J. BERNASCONI, S. SRASSLER, B. KNECHT, H. P. KLEIN and A. MENTH, *Solid State Commun.* **20** (1976) 1053.
17. K. EDA, *J. Appl. Phys.* **49** (1978) 2964.
18. G. D. MAHAN, L. M. LEVINSON and H. R. PHILIPP, *ibid.* **51** (1980) 4240.
19. L. K. J. VANDAMME and J. C. BRUGMAN, *ibid.* **52** (1980) 4240.
20. G. E. PIKE, "Electronic Properties of ZnO Varistors: A New Model", in "Grain Boundaries in Semiconductors," "Materials Research Society Proceedings", edited by H. J. Leamy, G. E. Pike and C. H. Seager (Materials Research Society, Pittsburg, PA, 1982) **5**, pp. 369-79.
21. J. T. C. VAN KEMENADE and R. K. EIJNTHOVEN, *J. Appl. Phys.* **50** (1979) 938.
22. O. L. KRIVANEK, P. WILLIAMS and Y. LIN, *ibid.* **50** (1979) 938.
23. E. M. LEVIN and R. S. ROTH, *J. Res. Natl. Bur. Stand. Sect. A* **68** (2) (1964) 19.
24. R. G. DOSCH, B. A. TUTTLE and R. A. BROOKS, *J. Mater. Res.* **1** (1986) 90.
25. T. J. GARDNER and S. J. LOCKWOOD, "Scale-Up of a Batch-Type Chemical Powder Preparation Process for High Field Varistor Fabrication", Sandia Report, SAND88-2194 (Sandia National Laboratories, Albuquerque, New Mexico, 1988) 76 pp.
26. *Idem.* "Sintering Schedule and Sample Geometry Effects on

- the Electrical and Physical Properties of High Field Varistor Materials", Sandia Report, SAND88-2449 (Sandia National Laboratories, Albuquerque, New Mexico, 1989) 53 pp.
27. K. M. KIMBALL and D. H. DOUGHTY, "Aluminum Doping Studies on High Field Varistors", Sandia Report, SAND86-0713 (Sandia National Laboratories, Albuquerque, New Mexico, 1987) 23 pp.
28. M. N. RAHAMAN and L. C. DE JONGHE, *J. Mater. Sci.* **22** (1987) 4326.

*Received 9 December 1988  
and accepted 10 April 1989*